Appl Magn Reson
DOI 10.1007/s00723-015-0734-8

Applied
Magnetic Resonance

The Sensitivity of Phosphocholine ^{13}C Chemical Shifts to pH

Ayelet Gamliel[1] · Netanel Chendler[1] · J. Moshe Gomori[1] · Jacob Sosna[1] · Rachel Katz-Brull[1]

Received: 26 July 2015 / Revised: 6 September 2015

Abstract Phosphocholine is a useful magnetic resonance (MR) biomarker for cancer. ^{13}C hyperpolarized MR is likely to enhance the detection of this compound by orders of magnitude. The ability to differentiate phosphocholine from its precursor, choline, in live tissues, is unique to MR and depends on the ^{13}C chemical shifts. The dependence of phosphocholine ^{13}C chemical shifts on pH was investigated. We found that under viable physiological conditions of $pH > 7$, the chemical shift of phosphocholine ^{13}C is stable and the chemical shift distance from the choline ^{13}C signals is preserved. Under acidic intracellular conditions of $6.0 < pH < 7$, the pH could be sensed by the phosphocholine ^{13}C chemical shifts. Crucial and damaging pH changes to values lower than 6.0 could be sensed at very high sensitivity. The highest precision for pH determination is obtained when considering the chemical shift difference between positions 1 and 2 of phosphocholine. The solution composition of human plasma did not affect the response of phosphocholine ^{13}C chemical shifts to pH.

1 Introduction

Choline (Cho) and phosphocholine (PCho) are the building blocks for membrane phospholipids, and in addition both have been identified as important molecular biomarkers. Radioactive Cho is a useful molecular imaging probe in positron emission tomography (PET) scans for cancer [1–3]. PCho is the product of Cho phosphorylation, catalyzed by the enzyme choline kinase (Fig. 1). PCho has been identified as an important magnetic resonance (MR) biomarker for cancer

✉ Rachel Katz-Brull
rkb@hadassah.org.il

[1] Department of Radiology, Hadassah-Hebrew University Medical Center, 91120 Jerusalem, Israel

Published online: 07 October 2015

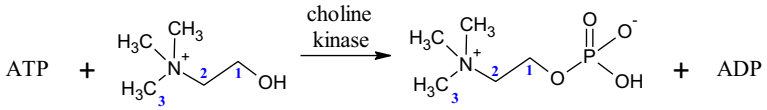

Fig. 1 Synthesis of phosphocholine (PCho) from choline (Cho) and adenosine triphosphate (ATP) catalyzed by the enzyme choline kinase. The carbon positions in Cho and PCho are marked by numerals

therapeutics [4–6], relying on the ability to differentiate PCho from Cho in live tissues, which is unique to MR. The total Cho metabolites signal seen on ^{1}H magnetic resonance spectroscopy (MRS), which is composed mainly of Cho, PCho, and glycerophosphocholine [7], and was also found to be a useful cancer marker and an indicator of treatment success [8, 9].

However, the utilization of these well-proven metabolic biomarkers has two major limitations. The major limitation of PET scans is the radiation associated with the radioactive nuclei within the Cho analog molecular imaging probe. As for clinical MRS examinations, the major limitation is the inherently low sensitivity of MR, detecting about 1 millionth of the actual nuclei present. Clinical MRS is applicable only at a very low spatial resolutions (of the order of centimeters) and low temporal resolutions (about 2–30 min per examination).

To overcome these two limitations, it may be useful to attempt the visualization of PCho with the hyperpolarized MR technology [10], as it enables a 10,000-fold increase in ^{13}C MR signal and is non-radioactive. We have previously shown that the longitudinal relaxation time of sp3 carbons in Cho can be prolonged by deuteration and that this enables visualization of Cho and its metabolites using hyperpolarized MR [11]. Hyperpolarized ^{13}C nuclei in Cho metabolites, namely acetylcholine, betaine aldehyde hydrate, and betaine, have been visualized and enabled the quantification of the rates of these metabolic conversions [11–15]. The ^{13}C label at Cho position 1 (Fig. 1) offers a chemical shift difference between Cho and PCho of about 2.4 ppm at a pH of 7 [12] and is therefore promising for visualization of PCho synthesis in a hyperpolarized state.

However, since PCho contains dissociable protons, the chemical shift of PCho nuclei is potentially pH dependent and therefore this chemical shift difference could be reduced and hinder the ability to differentiate PCho from Cho. Therefore, we have set to investigate the dependence of PCho ^{13}C chemical shifts on pH, as a preparation for possible future visualization of hyperpolarized PCho in live tissues.

The pH dependence of the chemical shift of the ^{31}P nucleus of PCho has been investigated before, and the pKa for PCho was determined [16]. However, this determination was made at 22 °C (as opposed to 37 °C which is relevant for live tissues) and in a different solution composition (which may affect the pKa). In addition, it is not possible to deduce the dependence of the ^{13}C nuclei chemical shifts from the ^{31}P chemical shift dependence on pH. To refer to the live tissue set-up, the pH dependence of ^{13}C chemical shifts was investigated in both aqueous solutions and human plasma.

2 Materials and Methods

2.1 Materials

Phosphocholine chloride calcium salt tetrahydrate and choline chloride were purchased from Sigma-Aldrich (Rehovot, Israel). Expired human plasma was donated by Hadassah Medical Center blood bank.

2.2 Solutions

Aqueous solutions: the concentration of Cho was 0.82 M and the concentration of PCho was 0.24 M. Human plasma: the concentration of Cho was 0.20 M and the concentration of PCho was 0.10 M. All of the plasma solutions were centrifuged, and the supernatant aspirated as a means to clear the solutions for NMR measurements. All measurements were carried out at a temperature of 37 ± 1 °C. Nine aqueous samples with pH ranging from 3.1 to 9.0 and nine plasma-based samples with pH ranging from 4.5 to 9.0 were scanned. It was not possible to obtain a plasma-based sample at a pH below 4.5 with suitable clarity for NMR measurement, as the samples clouded upon acidification below pH 4.5. The pH of the solutions was adjusted to the desired pH per sample with HCl and NaOH at 37 ± 1 °C. The ionic strength of the aqueous solutions was about 1.6 M, and the ionic strength of the plasma solutions could not be calculated due to the unknown ion composition of the sample.

2.3 NMR Measurements and Chemical Shift

NMR spectra of the solutions were recorded on a 500 MHz NMR spectrometer (Varian, Palo Alto, CA, USA) with a 5 mm ^{13}C direct probe. The ^{13}C chemical shifts were referenced to methanol at 49.5 ppm. The spectral resolution was 0.0038 ppm/point. Spectral processing was carried out using MNova (Mestrelab Research, Santiago de Compostela, Spain).

2.4 Processing of Chemical Shift Data to Obtain the pH Dependence Characteristics

Figure 4a and b shows the variation of the chemical shift with the solution pH for the ^{13}C nuclei of PCho at positions 1 and 2, respectively. The dependence of this shift on the pH showed the typical Henderson–Hasselbalch behavior, which can be described as $pH = pKa + \log[\delta_{obs} - \delta_1]/[\delta_2 - \delta_{obs}]$, if one assumes that a single pKa is present [$HA \rightarrow A^- + H^+$] [16], Ka is defined as $[A^-][H^+]/[AH]$, and here δ_{obs} is the chemical shift of a specific PCho ^{13}C position at a specific pH, δ_1 is the asymptotic chemical shift of this ^{13}C as the pH approaches negative infinity (very acidic), and δ_2 is the asymptotic chemical shift of this ^{13}C as the pH approaches infinity (very basic). The above equation was re-written as Eq. 1 (below) for convenience in further analysis [16].

Table 1 Characteristics of PCho ^{13}C chemical shift dependence on pH

	Based on position 1	Based on position 2	Based on the difference between position 1 and position 2
pKa[a]	5.58 (5.52, 5.65)	5.62 (5.42, 5.82)	5.60 (5.52, 5.67)
Sensitive pH range	4.19–6.98	4.23–7.01	4.20–6.99
Maximal change (ppm/pH units)	0.610	0.276	0.880
$\delta 1$[a]	59.47 (59.44, 59.49)	66.41 (66.37, 66.45)	–
$\delta 2$[a]	58.41 (58.39, 58.44)	66.89 (66.86, 66.92)	–
Derivative	$\delta'_{obs} = \frac{-2.44\times10^{pH-5.58}}{(1+10^{pH-5.58})^2}$	$\delta'_{obs} = \frac{1.11\times10^{pH-5.62}}{(1+10^{pH-5.62})^2}$	$\delta'_{obs} = \frac{3.52\times10^{pH-5.60}}{(1+10^{pH-5.60})^2}$

[a] Values are reported as fit results (95 % confidence interval)

The data were processed to extract the values of the pKa, the sensitive pH range, and the precision of pH determination in the following way. First, the data were fitted to Eq. 1 to estimate the pKa, δ_1, and δ_2. Then using these values the derivative of Eq. 1 was calculated (Eq. 2).

$$\delta_{obs} = \frac{\delta_1 + (\delta_2 \times 10^{pH-pKa})}{10^{pH-pKa} + 1} \quad (1)$$

$$\delta'_{obs} = \frac{\ln(10) \times (\delta_2 - \delta_1) \times 10^{pH-pKa}}{(1 + 10^{pH-pKa})^2} \quad (2)$$

The curves resulting from the fits of the entire data sets of positions 1 and 2 to Eq. 1 are shown by the solid lines in Fig. 4a, b, respectively, and the specific pKa, $\delta 1$, and $\delta 2$ values for each position are summarized in Table 1. The corresponding calculated derivatives are shown in these figures as dotted lines.

According to a methodology described by Vistad et al. [17] for ^{13}C NMR pH sensing, these derivatives serve to determine the sensitive range for pH determination or pH dependence. The maximal change of ppm/pH, calculated as the minimum or maximum of the derivative curve, is indicative of the precision of the pH determination within the sensitive pH range. The pH range in which a chemical shift is considered sensitive is defined as a pH range in which the ppm/pH change is above 15 % of this maximal change [17]. The resulting sensitive pH ranges and the maximal changes are summarized in Table 1.

2.5 Analysis of Chemical Shift Difference Data

The behavior of the chemical shift difference between position 1 and position 2 with pH was inspected as well. The resulting data (Fig. 5) were fitted to Eq. 3 (below), which was derived from Eq. 1.

$$\delta_{obs2} - \delta_{obs1} = \frac{\delta_{1,2} - \delta_{1,1} + (\delta_{2,2} - \delta_{2,1}) \times 10^{pH-pKa}}{10^{pH-pKa} + 1}, \quad (3)$$

where δ_{obs2} is the chemical shift of position 2; δ_{obs1} is the chemical shift of position 1 at a specific pH value;$\delta_{1,2}$ and $\delta_{1,1}$ are the asymptotic chemical shifts of positions

2 and 1, respectively, as the pH approaches negative infinity (very acidic, as determined in Sect. 2.4, Table 1); and $\delta_{2,2}$ and $\delta_{2,1}$ are the asymptotic chemical shifts of positions 2 and 1, respectively, as the pH approaches infinity (very basic, as determined in Sect. 2.4, Table 1). The resulting pKa, the sensitive pH range, and the maximal change for this chemical shift difference are summarized in Table 1.

2.6 Curve Fitting and Derivations

Curve fitting was performed using Matlab (MathWorks, Natick, MA, USA). Derivatives were calculated using Wolfram/alpha [18] and Matlab.

3 Results and Discussion

3.1 The pH Dependence of PCho ^{13}C Chemical Shifts

In aqueous solutions, PCho can be found in protonated and deprotonated forms (Fig. 2) with a distribution that depends on the pH. On ^{13}C spectra of the aqueous solutions, each PCho ^{13}C signal appears as a single resonance, at all pH values, suggesting that the protonated and deprotonated species are in fast exchange. These spectra (Fig. 3) also enable a distinct differentiation between the PCho and Cho ^{13}C signals of positions 1 and 2, as expected based on a previous characterization of the ^{13}C chemical shifts of these positions in these two compounds at a neutral pH [12]. This differentiation was maintained throughout the pH range investigated (pH 3.1–9.0). The difference in the chemical shift of the carbon at position 1 is the most significant one, ranging from 2.34 to 3.38 ppm. The differences observed for the carbon at position 2 ranged between 0.99 and 1.44 ppm. The signals of the carbons at position 3 of Cho and PCho overlapped with a small and pH-insensitive shift ($\sim$0.08 ppm). The finding that the magnitude of the change in chemical shifts of PCho was the greatest for position 1 was in agreement with the proximity of this position to the phosphate group in PCho, i.e., to the site where proton association or dissociation occurs (Fig. 2).

The reason for these differences in the PCho–Cho chemical shifts was that the PCho ^{13}C signals varied in chemical shift in response to a pH change. In a basic solution, the signal of the ^{13}C at position 1 of PCho is shifted to a lower frequency compared to the respective signal in an acidic solution (Fig. 3). In an opposing trend, the signal of the ^{13}C at position 2 of PCho is shifted to a higher frequency. The signal of the ^{13}C at position 3 of PCho did not show a change in chemical shift with pH. As opposed to PCho which contains dissociable protons, Cho does not.

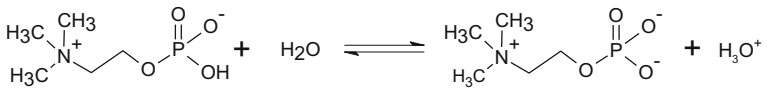

Fig. 2 pH-Induced equilibrium between protonated and deprotonated PCho

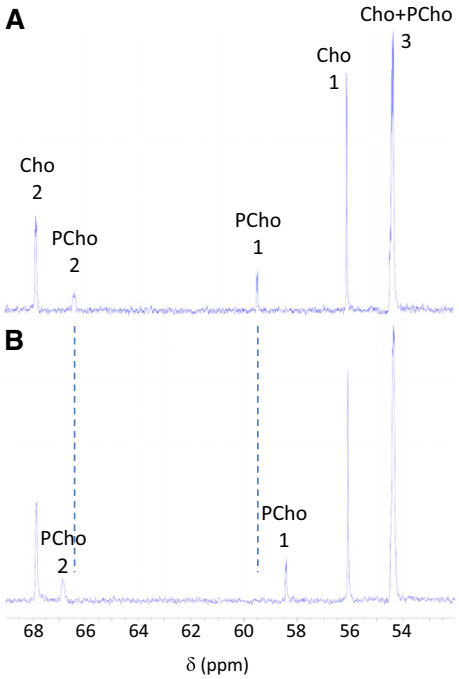

Fig. 3 ^{13}C NMR spectra of aqueous solutions containing choline (Cho) and phosphocholine (PCho) at 37 °C. The pH of the solutions was adjusted to 3.1 (**a**) and 9.0 (**b**) at 37 °C. The spectra were obtained by accumulating 256 (**a**) and 148 (**b**) transients with a 2 s repetition time and processed with a line broadening of 1 Hz (**a**) and 1.7 Hz (**b**)

Therefore, as expected, the chemical shift of the ^{13}C signals of Cho did not change between these two extreme pH conditions.

3.2 The Effect of Solution Composition and Temperature on the pH Dependence of PCho ^{13}C Chemical Shifts

The specific composition of a solution, its ionic strength, and the temperature may all affect the pKa of proton dissociation [16, 19, 20]. Specifically, for phosphates it has been shown that the ionic strength affects the pKa significantly [21], while changes in temperature lead to only slight or non-significant effects on pKa [22, 23]. For this reason, as a preparation for a potential examination in live tissues, the effect of pH on PCho ^{13}C chemical shifts was examined under two solution conditions: (1) aqueous solutions of PCho and Cho titrated with sodium hydroxide and hydrochloric acid represented solutions with a limited number of particle (ion) types; (2) solutions of PCho and Cho in human plasma, titrated with sodium hydroxide and hydrochloric acid, represented solutions with a composition that is biologically relevant. All solutions were titrated and scanned at 37 °C to match the temperature in live tissues, although the temperature does not seem to be a dominant factor affecting the pKa.

Figure 4a, b shows the variation of the chemical shift of PCho ^{13}C nuclei at positions 1 and 2, respectively, with the solution pH (in both solution types). The pattern of pH dependence of PCho ^{13}C chemical shifts was similar in the aqueous

and plasma solutions. Specifically, the pKa values for PCho, which were calculated from each data set (aqueous and plasma based) by a curve fit of the data of position 1 to the adapted Henderson–Hasselbalch equation (Eq. 1, Materials and Methods), were similar: 5.58 (95 % CI 5.42–5.73) and 5.63 (95 % CI 5.53–5.74), respectively. The similarity of these two values suggested that the results from both solution types could be combined for further analysis. We concluded that the plasma solution composition does not contain factors that affect the response of PCho ^{13}C chemical shifts to pH, as measured in aqueous solutions of limited particle types.

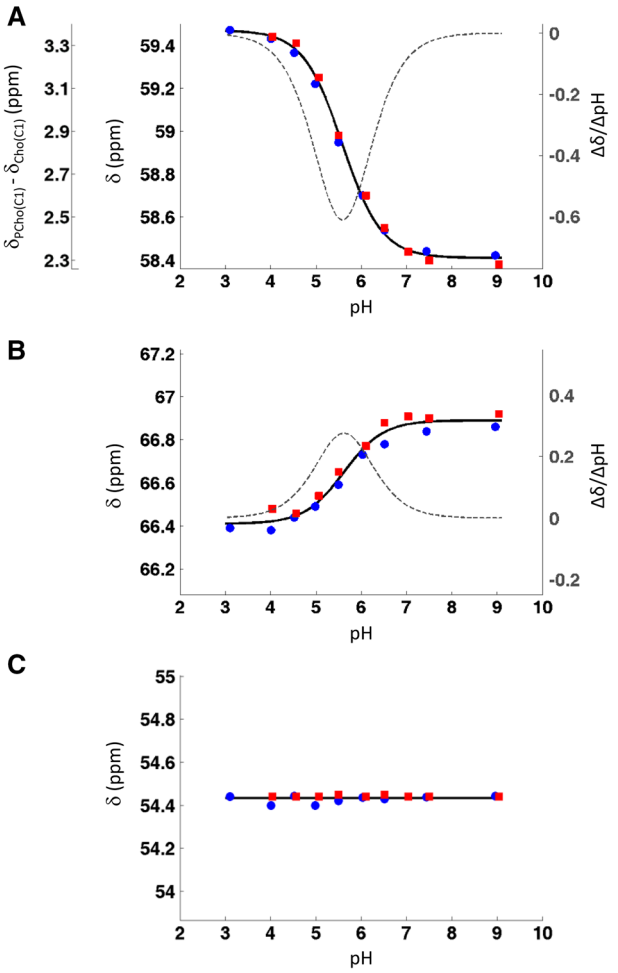

Fig. 4 **a**, **b** The chemical shift, δ (ppm), of the PCho ^{13}C nuclei at positions 1 and 2, respectively, under varying pH values. The solid lines show the fits to Eq. 1. The dotted lines depict the derivatives of these curves (Eq. 2) and relate to the vertical axes on the right (Δδ/ΔpH units). **c** The δ of the ^{13}C nucleus at position 3 of PCho under varying pH values. The *red squares* represent results determined in plasma-based samples. *Blue circles* represent results obtained in aqueous solutions

The insensitivity of the chemical shift of position 3 (trimethylamine carbons) across the investigated pH range in both solution types is depicted in Fig. 4c.

3.3 Analysis of pKa, Sensitive pH Range, and Precision for Positions 1 and 2

The data were further processed to extract the values of pKa, sensitive pH range, and precision of pH determination from each plot (Fig. 4a, b) as described in Sect. 2.4. The calculated pKa (5.6) and the sensitive pH range (4.2–7.0) were found to be the same for both position 1 and position 2 of PCho (Table 1), although the direction and magnitude of the change in chemical shift were different. The similarity in these calculated values is to be expected, as they reflect the same chemical change in the same molecule. This pKa value was close to a previous determination which reported a value of 5.76 ± 0.03, based on PCho ^{31}P chemical shifts [16]. We suggest that the differences in solution composition between the current and the previous determination may have led to the 0.1–0.2 pH units difference in pKa. The ionic strength in the current solutions was high due to the NMR sensitivity requirements. The previous study also used solutions with high ionic strength. However, due to the use of aminopolycarboxylic acid compounds, such as EDTA, the ionic strength of these solutions was dependent on pH, prohibiting comparison to the current study in this aspect.

3.4 Analysis of the Difference Between Positions 1 and 2

Because the change in the chemical shifts of positions 1 and 2 with pH was in opposite directions, it raised the possibility that the chemical shift difference between the two positions may offer better precision of the pH determination. For this reason, the behavior of this chemical shift difference against pH was inspected as well. The data (Fig. 5) were processed as described in the Sect. 2.5. The pKa and the sensitive pH range calculated from these data were the same as those calculated

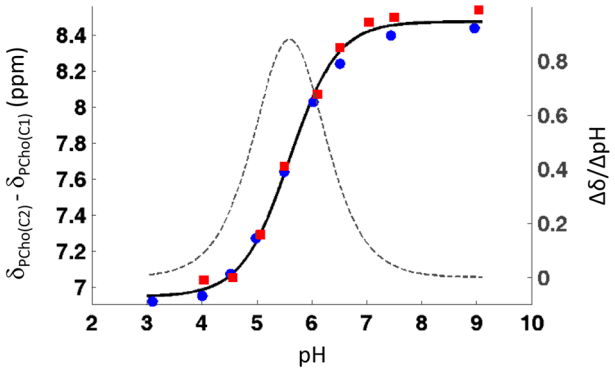

Fig. 5 Chemical shift difference between position 1 and position 2 of PCho under varying pH values. The *solid line* shows the fit to Eq. 3. The *dotted line* depicts the derivative of this *curve* and relates to the *vertical axis* on the right (Δδ/ΔpH)

for each position alone. However, the precision of the pH determination within the sensitive pH range, expressed as the maximal change in ppm/pH, was indeed higher (0.880 ppm/pH) than that of each position alone (0.61 and 0.28 ppm/pH for positions 1 and 2, respectively).

3.5 Implications of our Findings to Experiments in Live Tissues

3.5.1 Expected variation of PCho ^{13}C Chemical Shifts in Live Tissues

In cellular compartments, the pH ranges from 7.2 to 7.8 (e.g., cellular cytosol and mitochondrial matrix, respectively). Under such conditions (and for higher pH values), it is expected that all of PCho chemical shift indicators (position 1, position 2, and the difference between them) will be constant. However, for biological conditions in which the pH is lower than 7.0, for example tumor microenvironment in which the pH can range from 6.0 to 6.5, PCho chemical shifts will indicate this change. This partition into two different regimes, one in which the PCho protonation status is constant and another in which PCho protonation varies, was recently utilized to target PCho-containing copolymers to tumor microenvironment [24], in agreement with the current findings.

3.5.2 pH Sensing

pH sensing using chemical shift changes has been reported for numerous compounds and nuclei. pH sensing via ^{13}C chemical shift changes are less commonly reported, most likely due to the lower sensitivity of ^{13}C MRS compared to ^{1}H or ^{31}P MRS. Nevertheless, with the advent of ^{13}C hyperpolarized MR and numerous ^{13}C-labeled compounds that are being developed for this technology [25], it is likely that more studies on this topic will evolve.

Of note here is the investigation into the pH-sensing properties of ^{13}C-bicarbonate by hyperpolarized MR. Bicarbonate is the main extracellular buffer, helping in the control of acid–base balance in the body through the exchange between bicarbonate (HCO_3^-) and carbon dioxide (CO_2) catalyzed by carbonic anhydrase [26]. The distribution between the two species depends upon pH (according to the Henderson–Hasselbalch equation), and hence the ratio between the two can be translated into the pH of the tissue examined (specifically extracellular pH since bicarbonate is mainly an extracellular buffer) [27]. The bicarbonate probe was the first demonstration of pH determination using molecular imaging probes that contain hyperpolarized ^{13}C nuclei [26].

Our study suggests that under viable physiological conditions of pH > 7 and 37 °C, the ^{13}C chemical shift of PCho, which is mostly intracellular, is not expected to vary and the chemical shift difference from the Cho ^{13}C signals is expected to be preserved. Under acidic intracellular conditions of $6.0 <$ pH < 7, the pH could be sensed by the PCho ^{13}C chemical shifts, where the precision would be the highest when the chemical shift difference between positions 1 and 2 is used. Crucial and damaging pH changes to values lower than 6.0 could be sensed at very high sensitivity.

Acnowledgments This work was funded by the Israel Science Foundation (Grant No. 284/10) and the European Research Council (Grant No. 338040).

References

1. T. Hara, T. Kondo, T. Hara, N. Kosaka, J. Neurosurg. **99**(3), 474–479 (2003)
2. K.B. Contractor, L.M. Kenny, J. Stebbing, A. Al-Nahha, C. Palmieri, D. Sinnett, J.S. Lewis, K. Hogben, S. Osman, S. Shousha, C. Lowdell, R.C. Coombes, E.O. Aboagye, Clin. Cancer Res. **15**(17), 5503–5510 (2009)
3. T.H. Witney, I.S. Alam, D.R. Turton, G. Smith, L. Carroll, D. Brickute, F.J. Twyman, Q.D. Nguyen, G. Tomasi, R.O. Awais, E.O. Aboagye, Clin. Cancer Res. **18**(4), 1063–1072 (2012)
4. H.S. Venkatesh, M.M. Chaumeil, C.S. Ward, D.A. Haas-Kogan, C.D. James, S.M. Ronen, Neuro-Oncology **14**(3), 315–325 (2012)
5. R. Katz-Brull, D. Seger, D. Rivenson-Segal, E. Rushkin, H. Degani, Cancer Res. **62**(7), 1966–1970 (2002)
6. N.M. Loening, A.M. Chamberlin, A.G. Zepeda, R.G. Gonzalez, L.L. Cheng, NMR Biomed. **18**(7), 413–420 (2005)
7. R. Katz-Brull, A.R. Koudinov, H. Degani, Brain Res. **951**(2), 158–165 (2002)
8. R. Katz-Brull, P.T. Lavin, R.E. Lenkinski, J. Natl. Cancer Inst. **94**(16), 1197–1203 (2002)
9. B.F. Jordan, K. Black, I.F. Robey, M. Runquist, G. Powis, R.J. Gillies, NMR Biomed. **18**(7), 430–439 (2005)
10. J.H. Ardenkjaer-Larsen, B. Fridlund, A. Gram, G. Hansson, L. Hansson, M.H. Lerche, R. Servin, M. Thaning, K. Golman, Proc. Natl. Acad. Sci. USA **100**(18), 10158–10163 (2003)
11. H. Allouche-Arnon, M.H. Lerche, M. Karlsson, R.E. Lenkinski, R. Katz-Brull, Contrast Media Mol. Imaging **6**, 499–506 (2011)
12. H. Allouche-Arnon, A. Gamliel, C.M. Barzilay, R. Nalbandian, J.M. Gomori, M. Karlsson, M.H. Lerche, R. Katz-Brull, Contrast Media Mol. Imaging **6**, 139–147 (2011)
13. H. Allouche-Arnon, A. Gamliel, J. Sosna, J.M. Gomori, R. Katz-Brull, Chem. Commun. **49**(63), 7076–7078 (2013)
14. H. Allouche-Arnon, Y. Hovav, L. Friesen-Waldner, J. Sosna, J.M. Gomori, S. Vega, R. Katz-Brull, NMR Biomed. **27**(6), 656–662 (2014)
15. L.J. Friesen-Waldner, C.N. Wiens, T.P. Wade, K. Thind, K.P. Sinclair, Y. Hovav, J.M. Gomori, J. Sosna, C.A. McKenzie, R. Katz-Brull, Chem. Commun. **50**(89), 13801–13804 (2014)
16. P.M.L. Robitaille, P.A. Robitaille, G.G. Brown, J. Magn. Reson. **92**(1), 73–84 (1991)
17. O.B. Vistad, D.E. Akporiaye, F. Taulelle, K.P. Lillerud, Chem. Mat. **15**(8), 1650–1654 (2003)
18. Wolfram/alpha, (http://www.wolframalpha.com)
19. J.N. Butler, *Solubility and pH Calculations : the Mathematics of the Simplest Ionic Equilibria* (Addison-Wesley, Boston, 1964)
20. J.N. Butler, *Ionic Equilibrium : a Mathematical Approach* (Addison-Wesley, Boston, 1964)
21. D.G. Gadian, Biological applications of magnetic resonance, Chapter 10. 31P NMR in living tissue, ed. by R.G. Shulman (Academic Press, New York, 1979)
22. R.K. Scopes, Protein purification; principles and practice, Chapter 12.3 Control of pH: Buffers. Springer advanced texts in chemistry. 3rd edn. (Springer, New York, 1994)
23. E. Humeres, J. Quijano, M.M.S. de Siera, J. Braz. Chem. Soc. **1**(3), 99–104 (1990)
24. X.F. Yu, X.Q. Yang, S. Horte, J.N. Kizhakkedathu, D.E. Brooks, Biomaterials **35**(1), 278–286 (2014)
25. K.R. Keshari, D.M. Wilson, Chem. Soc. Rev. **43**(5), 1627–1659 (2014)
26. F.A. Gallagher, M.I. Kettunen, S.E. Day, D.-E. Hu, J.H. Ardenkjaer-Larsen, R. in't Zandt, P.R. Jensen, M. Karlsson, K. Golman, M.H. Lerche, K.M. Brindle, Nature **453**(7197), 940–943 (2008)
27. F.A. Gallagher, M.I. Kettunen, S.E. Day, D.-E. Hu, M. Karlsson, A. Gisselsson, M.H. Lerche, K.M. Brindle, Magn. Reson. Med. **66**(1), 18–23 (2011)